Model of an Asymmetric DPPC/DPPS Membrane: Effect of Asymmetry on the Lipid Properties. A Molecular Dynamics Simulation Study

J. J. López Cascales,*,† T. F. Otero,† Bradley D. Smith,‡ Carlos González,§ and M. Márquez|,§

Universidad Politécnica de Cartagena, Centro de Electroquíca y Materiales Inteligentes (CEMI), Aularío II, Campus de Alfonso XIII, 30203 Cartagena, Murcia, Spain, Department of Chemistry and Biochemistry, University of Notre Dame, Notre Dame, Indiana 46556, National Institute of Standards and Technology (NIST), Building 221, Room A111, Gaithersburg, Maryland 20899, Chemistry Division, Los Alamos National Laboratory, Los Alamos, New Mexico 87545, and I'NEST Group, New Technology Research, PMUSA, Richmond, Virginia 23234

Received: October 31, 2005; In Final Form: December 13, 2005

The study of asymmetric lipid bilayers is of a crucial importance due to the great number of biological process in which they are involved such as exocytosis, intracellular fusion processes, phospholipid−protein interactions, and signal transduction pathway. In addition, the loss of this asymmetry is a hallmark of the early stages of apoptosis. In this regard, a model of an asymmetric lipid bilayer composed of DPPC and DPPS was simulated by molecular dynamics simulation. Thus, the asymmetric membrane was modeled by 264 lipids, of which 48 corresponded to $DPPS^-$ randomly distributed in the same leaflet with 96 DPPC. In the other leaflet, 120 DPPC were placed without $DPPS^-$. Due to the presence of a net charge of −1 for the $DPPS^-$ in physiological conditions, 48 Na^+ were introduced into the system to balance the charge. To ascertain whether the presence of the $DPPS^-$ in only one of the two leaflets perturbs the properties of the DPPC in the other leaflet composed only of DPPC, different properties were studied, such as the atomic density of the different components across the membrane, the electrostatic potential across the membrane, the translational diffusion of DPPC and DPPS, the deuterium order parameters, lipid hydration, and lipid−lipid charge bridges. Thus, we obtained that certain properties such as the surface area lipid molecule, lipid head orientation, order parameter, translational diffusion coefficient, or lipid hydration of DPPC in the leaflet without DPPS remain unperturbed by the presence of DPPS in the other leaflet, compared with a DPPC bilayer. On the other hand, in the leaflet containing DPPS, some of the DPPC properties were strongly affected by the presence of DPPS such as the order parameter or electrostatic potential.

1. Introduction

Biological membranes are crucial cellular components with multiple roles. For example, they maintain electrochemical gradients by controlling the diffusion of ions and biomolecules, they act as a supporting matrix for embedded enzymes and receptors, and they engage in stabilizing interactions with skeletal proteins. It is becoming increasingly clear that biological membranes are a complex and heterogeneous assembly of nonpolar and amphiphilic molecules and that theoretical methods will play an important role in developing an atomic-scale picture of the structure and kinetics of membrane assembly.

In this regard, the past decade has seen the first attempts to simulate the structure of highly simplified bilayer membranes. These pioneering studies have typically employed the molecular dynamics (MD) technique to study a homogeneous bilayer membrane composed of one type of phospholipid. In 1994, Egberts et al.[1] carried out preliminary studies of DPPC (DPPC: dipalmitoylphosphatidylcholine) bilayers, in which they identified various phospholipid−phospholipid and phospholipid−water interactions that formed the basis of the assembly. They also estimated the rate of water diffusion across the bilayer. Subsequent studies of other bilayer systems have employed analogous methodology. Cascales et al.[2,3] carried out simulations of a bilayer composed of an anionic DPPS (DPPS: dipalmitoylphosphatidylserine) bilayer (compared with the DPPC membrane which is uncharged in physiological conditions), the surface of which is smaller, even when it is highly anionic. The simulations of DPPS bilayers provided useful information concerning the most likely phospholipid−phospholipid interactions and the effect of the charged bilayer on the water structure in the vicinity of the membrane surface.

In recent years, growing computing power and improved simulation algorithms have led to more complicated simulations and extended the trajectory length. Thus, for example, Pandit et al.[4] studied the effect of salt concentration on the structure of a DPPC bilayer and lipid complexation and ion binding in symmetric mixed bilayers of DPPC and DPPS.[5] Mukhopadhyay et al.[6] carried out several MD simulations of a palmitoyloleoylphosphatidylserine (POPS) bilayer with sodium counterions and additional sodium chlorides. Sach et al.[7] also studied the changes in phospholipid headgroup tilt induced by the presence of monovalent salts.

However, the common denomination of all the works mentioned above was the use of symmetrical bilayers that have an equal number and the same type of phospholipids in each leaflet of the membrane. However, it is well-known that the

* To whom correspondence should be addressed: javier.lopez@upct.es.
† Centro de Electroquíca y Materiales Inteligentes (CEMI).
‡ University of Notre Dame.
§ National Institute of Standards and Technology (NIST).
|| Los Alamos National Laboratory and I'NEST Group.

10.1021/jp0562680 CCC: $33.50
Published on Web 01/17/2006

distribution of phospholipids across most, if not all, animal membranes is asymmetric.[8] In particular, the external side of animal plasma membranes is enriched with zwitterionic phospholipids such as phosphatidylcholine (PC), whereas the internal side is enriched in aminophospholipids such as phosphatidylserine (PS). This asymmetric distribution is a central part of normal cell functioning. For example, the PS that is normally located on the inside of the plasma membrane is vital not only for exocytosis and intracellular fusion processes but also for phospholipid−protein interactions and the signal transduction pathway.[9] Furthermore, the loss of phospholipid membrane asymmetry is a hallmark of the early stages of cell apoptosis. In particular, the appearance of PS on the outside of the membrane triggers cell clearance by phagocytosis,[10,11] a process whereby apoptotic cells are removed from the bloodstream by macrophages that specifically recognize the PS on the cell surface.[12] In healthy cells, transmembrane asymmetry is maintained by the concerted action of phospholipid translocase enzymes that vary in lipid specificity, energy requirements, and the direction of translocation. The translocases can be divided into three classes: bidirectional "scramblases" and energy-dependent transporters that move phospholipids toward ("flippases") or away from ("floppases") the inner surface of the membrane. At present, it is not known how translocase enzymes operate at the molecular level. In the absence of translocase enzymes, spontaneous phospholipid translocation (also known as flip-flop) is a very slow process that can be promoted by treatment with organic compounds that lower the activation barrier by diminishing headgroup polarity[13] or by forming water filled channels.[14]

The goal of the present theoretical study was to conduct molecular dynamics simulations of a bilayer membrane with an asymmetric distribution of phospholipids, with the aim of elucidating how this asymmetry is propagated from one leaflet to the other one. As a simplified copy of the typical arrangement in a healthy animal plasma membrane, one leaflet was composed of pure DPPC, thus being uncharged, whereas the opposite leaflet included some $DPPS^-$ and was, thus, anionic. The studies probed the effect of asymmetric phospholipid distribution on membrane properties such as phospholipid headgroup hydration, membrane electrostatic potential, membrane fluidity, and phospholipid diffusion.

The model of lipid membrane proposed in this work may be used for further studies where asymmetry plays an important role in the behavior of the system, such as proteins or anaesthetic molecules embedded into an asymmetric membrane.

2. Method and Model

2.1. Setting up the System. Two computer simulations were carried out in this work: (1) a DPPC bilayer in water, divided into two layers of 144 DPPC lipids each and (2) 216DPPC/48DPPS/48Na^+ in water, split into two leaflets of 120 DPPC in the first leaflet and 48 DPPS plus 96 DPPC in the second.

2.1.1. DPPC Bilayer in Water. A three dimension periodical system was generated, starting from a single DPPC molecule (Figure 1) placed perpendicularly to the water layer. This single DPPC molecule was randomly rotated and replicated on two leaflets of 144 DPPC molecules each (288 DPPC in total). The gap existing in the generated computing box was filled in with 10 054 water molecules from a steady and well-equilibrated computing box of water of the SPCE water model.[15]

2.1.2. 216DPPC/48DPPS/48Na^+ in Water. The system was generated starting from a DPPC bilayer with 144 DPPC in each leaflet, such as was explained in the previous section 2.1.1. Then,

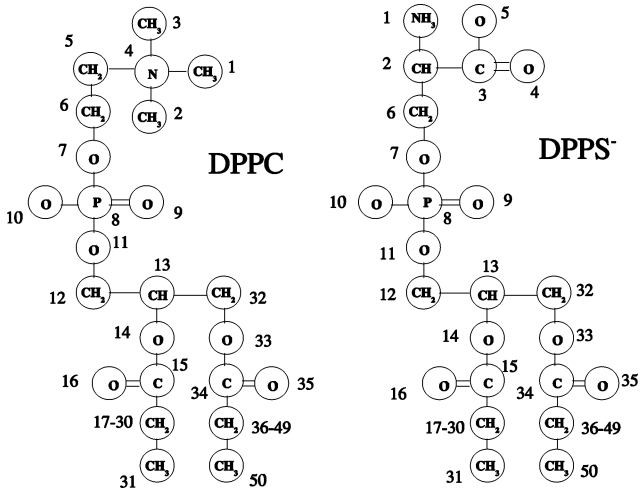

Figure 1. Atomic numeration of a single DPPC and DPPS lipid, such as they will be referred to throughout this article.

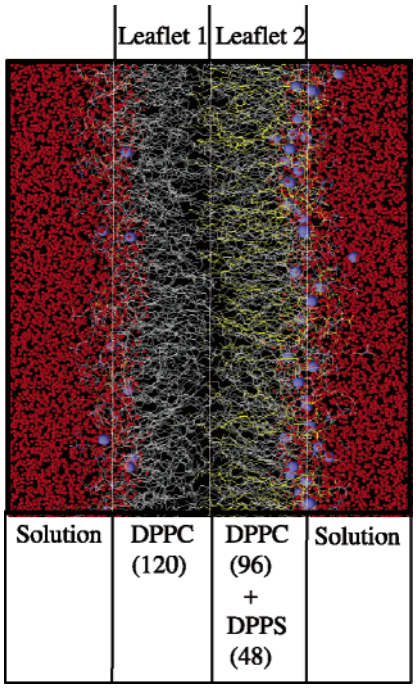

Figure 2. Snapshot of the DPPC + DPPS bilayer. Big beads correspond to sodium ions (Na^+), and small beads correspond to water molecules. DPPS is plotted in yellow, and DPPC is in gray wireframes.

48 DPPC were randomly substituted by 48 DPPS (Figure 1) in only one of the two lipid leaflets. In the other leaflet, 24 DPPC molecules were removed in order to fit the surface area and mass density of a pure DPPC bilayer, thus avoiding an excess of surface pressure in the DPPC leaflet that could introduce undesired simulation artifacts. After modeling the system, 48 water molecules were substituted by 48 Na^+, following a minimization electrostatic energy criteriom, which produced a charge-neutral system. In this way, the DPPS represented 18% of the total number of lipids of the system, which is near the lipid composition of some subcellular membranes.[8] Figure 2 depicts a snapshot of the system thus generated.

2.2. Starting up the Simulations. The GROMACS 3.1.4 package[16,17] was used as an engine to carry out our simulations. The force field parameters and electrostatic charge distribution of the DPPC and DPPS were the same as those used by Egberts et al.[1] and Cascales et al.[2] in previous simulations of pure bilayers of DPPC and DPPS in their liquid crystalline state,

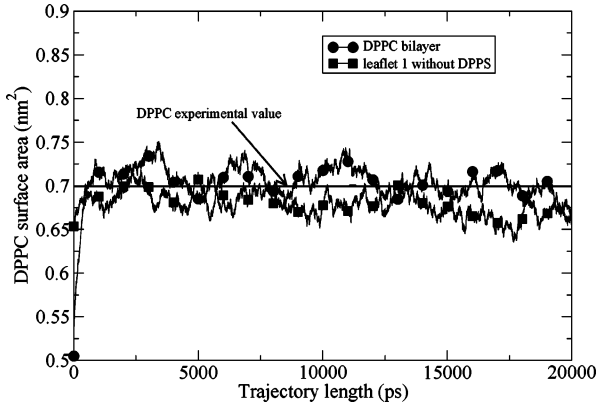

Figure 3. DPPC area running along the simulated trajectory.

respectively. A cutoff of 1.0 nm was used for calculating the Lennard−Jones interactions. The electrostatic interactions were evaluated using the particle mesh Ewald method.[18,19] The real space interactions were evaluated using a 0.9 nm cutoff, and the reciprocal space interactions were evaluated on a 0.12 nm grid with a fourth-order spline interpolation.

The two systems were subjected to a steepest descent energy minimization procedure to remove undesired overlapping between neighboring atoms. Once the two systems had reached a minimum of potential energy, each system was launched on a 500 ps simulation at a temperature of 500 K to remove any undesired interaction between neighboring lipids. In this case, the leap frog integrator algorithm was used, with a time step of 4 fs. Each component of the system was coupled to an external temperature coupling bath of 0.1 ps and to an anisotropic pressure external bath of 1 atm, with a coupling constant of 0.5 ps.[20] After running 500 ps of simulations at 500 K, the systems were cooled in the two cases to 350 K, which is well above the transition temperatures of 314 K and 326 K for the DPPC[21,22] and DPPS[23,24] bilayers, respectively. Then, a trajectory length of 20 ns was carried out.

Figure 3 shows the variation of the surface area per DPPC molecule, calculated from the leaflet containing only DPPC molecules and from the pure DPPC bilayer in water. From simulation, we observe how, after 5000 ps of simulations, the surface area achieved a steady state in perfect accordance with the previous simulations of de Vries et al.[25] for a DPPC bilayer of 36 DPPC/leaflet and Mukhopadhyay et al.[6] and Pandit et al.[5] for simulations of POPS and DPPC, respectively, in the presence of salt. Data from the last 15 ns of the total simulated trajectory were used to extract the properties that are presented in this work.

All the simulations were carried out on a node with four processors of a parallel HP ES 45 cluster Alpha Server, where 1 month of intensive computing time was required for each one of the two simulations carried out in this work.

3. Results

3.1. Membrane Structure. *3.1.1. Surface Area.* The area of the computing box divided by the number of lipids per leaflet along the simulated trajectory gives a DPPC surface area of 0.703 ± 0.015 nm^2 (Figure 3). Even considering the wide range of values for the surface area of DPPC bilayers, such as depicted in the revision by Tristram-Nagle et al.,[26] our results are in perfect agreement with the value of 0.70 nm^2 reported from experimental measurements[27,28] for a temperature of 350 K. When DPPS$^-$ was asymmetrically introduced into only one of the two leaflets, the DPPC surface area was 0.68 ± 0.02 nm^2,

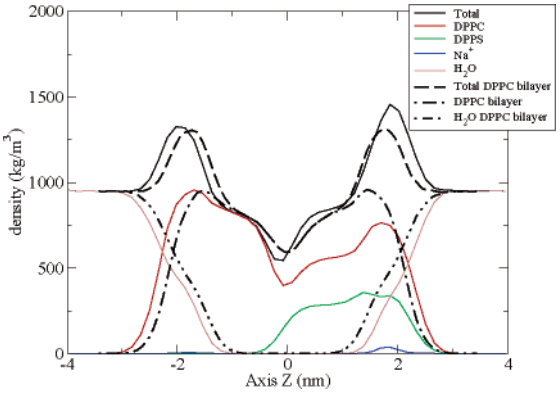

Figure 4. Mass density across the asymmetric lipid bilayer. The density of the pure DPPC bilayer is included as reference.

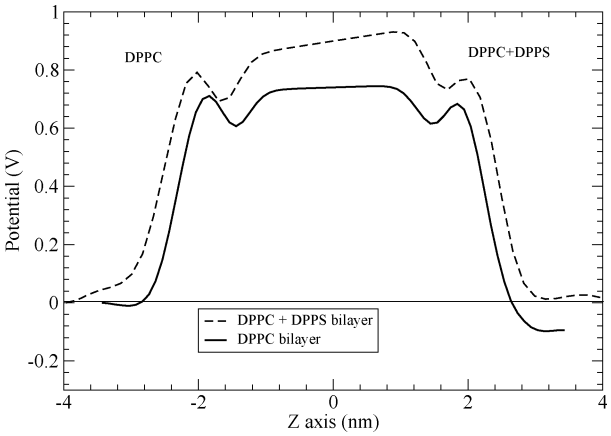

Figure 5. Electrostatic potential across the lipid bilayers.

which also reproduces (considering the error bar) the surface area of a DPPC bilayer.

3.1.2. Mass Density across the Lipid Bilayer. Figure 4 displays the mass density across the phospholipid bilayers. In addition, these figures were compared with the DPPC bilayer in order to see how the density is affected by the presence of DPPS asymmetrically distributed in the bilayer.

Figure 4 also shows that the asymmetry due to the presence of DPPS$^-$ introduces phospholipid dehydration on both leaflets of the membrane, compared with a symmetric DPPC bilayer. This appears to be due to sodium ions displacing solvating water molecules and cross-linking neighboring phospholipids. Finally, the asymmetry in the bilayer induces a gradient in the total atomic density, so that the total density in the leaflet containing the DPPS is higher than that in the leaflet composed only of DPPC molecules.

3.1.3. Electrostatic Potential across the Lipid Bilayer. The electrostatic potential ψ across the asymmetric bilayer was computed from the simulation by a numerical evaluation of the double integral of the charge density (ρ) across the bilayer[29] as follows:

$$\psi(z) - \psi(0) = -\frac{1}{\epsilon_0}\int_0^z dz' \int_0^{z'} \rho(z'')\, dz'' \qquad (1)$$

where the origin z of the potential $\psi(0)$ is taken at the middle of the water layer. We are aware that the electrostatic potential computed in this way is consistent with the computed charge density using Poisson's equation, without using a cutoff radius.[4]

Figure 5 shows the electrostatic potential across the asymmetric bilayer. As we can observe from Figure 5, even when the charge carried by the DPPS$^-$ is balanced by the presence

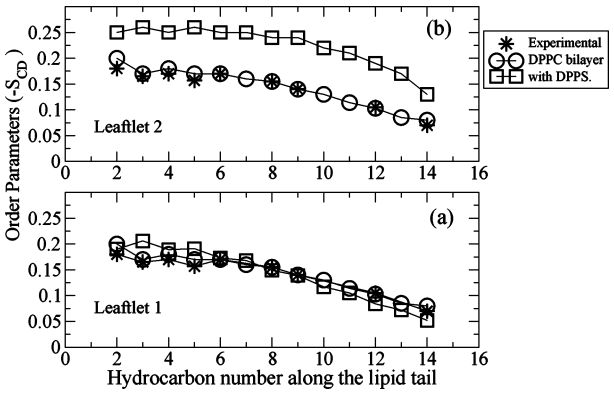

Figure 6. DPPC order parameter for both lipid monolayers: (a) leaflet 1 without DPPS; (b) leaflet 2 with DPPS. The symbol ○ refers to our simulation results of the pure DPPC bilayer, and ∗refers to the experimental results of a pure DPPC bilayer.[31]

of sodium, the presence of this ion is unable to completely screen the net charge associated with the $DPPS^-$ and, as a consequence, an electrostatic gradient between both leaflets of the membrane emerges.

3.1.4. Deuterium Order Parameter. The deuterium order parameter (S_{CD}) has been widely used to characterize the structure of the hydrocarbon region inside a lipid bilayer. This property can be extracted from the simulation as follows:

$$S_{CD} = \frac{2S_{xx}}{3} + \frac{S_{yy}}{3} \tag{2}$$

where S_{xx} and S_{yy} are the terms of the order parameter tensor **S** defined as

$$S_{\alpha\beta} = \frac{\langle 3\cos\theta_\alpha \cos\theta_\beta - \delta_{\alpha\beta}\rangle}{2}; \quad \alpha = x, y, z, \beta = x, y, z \tag{3}$$

where θ_i is the angle between the ith molecular axis and the normal to the bilayer and $\delta_{\alpha\beta}$ is the Kronecker delta. The x and y axes of the bilayer were taken on the membrane plane, while z is normal to the membrane plane. A more detailed description can be obtained from the articles cited in refs 2 and 30. In our case, the order parameters discussed below were averaged over both hydrocarbon lipid tails.

The order parameter data in Figure 6 show excellent agreement between the simulation and experimental results[31] for a DPPC bilayer at a temperature of 350 K. In addition, the bilayer order increased in the presence of DPPS, an effect which was particularly noticeable in the leaflet containing DPPS. Thus, for the leaflet containing only DPPC, there was perfect agreement with the experimental values, except for the first atoms of the hydrocarbon tails for which a slight increase was observed. These results can be considered clear evidence that no simulation artifact, such an excess of pressure on any of the two leaflets of the membrane, existed to distort the results. On the other hand, for the leaflet containing DPPS, the presence of DPPS increased the order parameter of the DPPC.

Figure 7 compares variations in the simulated and experimental order parameters of the DPPS hydrocarbon tails.[32] In this case, unlike in the results obtained for DPPC, almost no variations in the order parameters were observed for the DPPS embedded in the leaflet containing DPPC, compared with the experimental values obtained for a bilayer composed only of DPPS. This result, too, allows us to assert that there were no simulation artifacts that could perturb our conclusions, such as

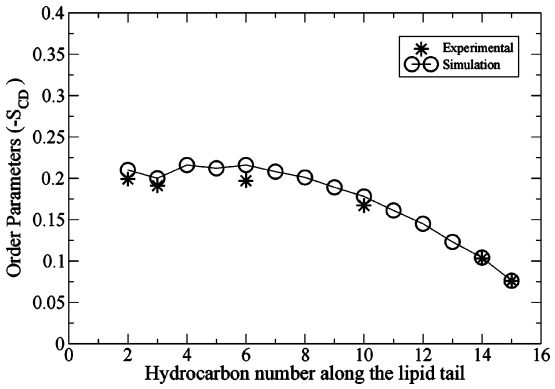

Figure 7. DPPS order parameter. The symbol ∗refers to the experimental results.[32]

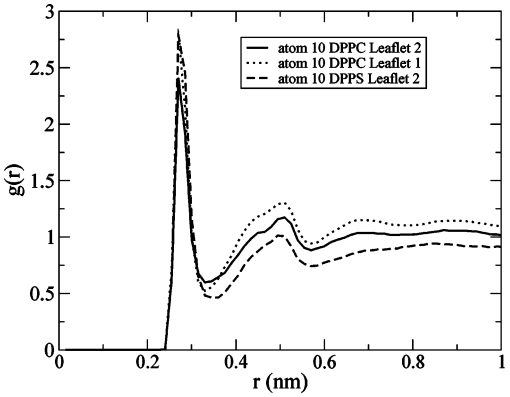

Figure 8. Radial distribution function $g(r)$ of water−oxygen around the carboxyl phosphate group (atom 10) of DPPC and DPPS.

a greater pressure associated with an excess of lipid packaging compared with the other leaflet.

3.1.5. Radial Distribution Function. The radial distribution function $g(r)$ is often employed to identify close interactions between neighboring atoms. In this regard, the radial distribution function $g(r)$ is defined as

$$g(r) = \frac{N(r)}{4\pi r^2 \rho \delta r} \tag{4}$$

where $N(r)$ is the number of atoms in a spherical shell at a distance r and thickness δr from a reference atom and ρ is the number density taken as the ratio of atoms to the volume of the computing box.

To analyze the hydration of the two types of lipids in both membrane leaflets, we calculated the $g(r)$ around one of the two oxygens of the phosphate oxygen group (atom number 10 in Figure 1). Thus, from Figure 8, we observe how the peak of the radial distribution function of the DPPS is higher than that for DPPC on both leaflets of the membrane.

From numerical integration of the area under the first peak of the radial distribution function, we are able to obtain the hydration numbers around atom 10 (phosphate oxygen) of the DPPC. With the goal of measuring the error bar of the hydration numbers, the trajectory file was split up into four subtrajectories of 5 ns length each (where the first subtrajectory was discarded for the statistic). Thus, the value of 2.06 ± 0.06 was obtained for the above-mentioned atom of DPPC in the leaflet without DPPS and 1.96 ± 0.05 was obtained for the DPPC in the leaflet with DPPS. As regards DPPS, we obtained the hydration number of 2.13 ± 0.07 for the same atom number. Our simulations indicate that the DPPS is slightly more hydrated than the DPPC.

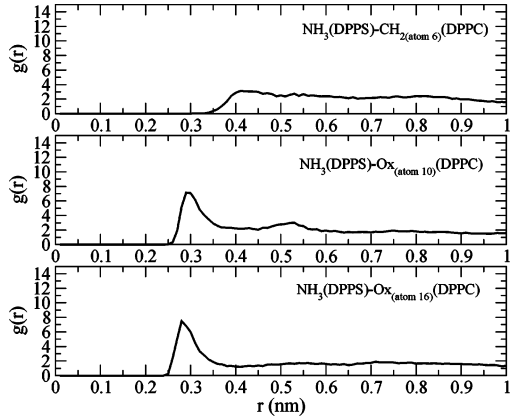

Figure 9. Radial distribution function of several DPPC oxygens around the NH_3 of DPPS.

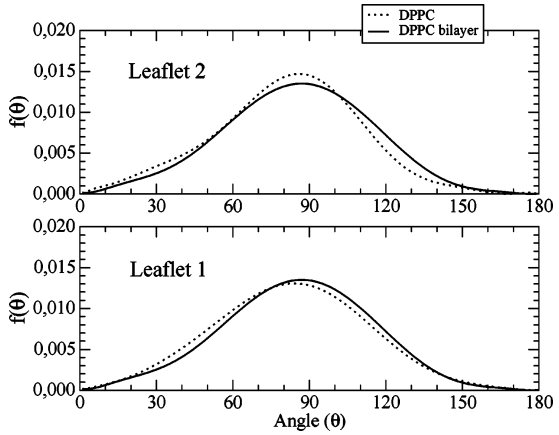

Figure 10. Distribution of the angle between the vector joining the **P**−**N** vector of DPPC and the outward normal of the bilayer on both asymmetric phospholipid monolayers. Monolayer 2 corresponds to the lipid layer composed by DPPC + DPPS, and monolayer 1 corresponds to the layer formed only by DPPC.

On the other hand, we can conclude that DPPC dehydration is unperturbed by the presence of DPPS.

In addition, the radial distribution function $g(r)$ was also used to identify charge bridges between neighboring phospholipids. Thus, the NH_3 of the DPPS (atom 1 from Figure 1) was assigned as the reference atom to calculate the radial distribution function and several atoms of the DPPC were assigned as the coordination atoms. Figure 9 depicts the radial distribution function of three different DPPC atoms around the NH_3 group: the CH_2 of the choline headgroup (atom 6, Figure 1), the phosphate oxygen (atom 10, Figure 1), and the carbonyl oxygen group (atom 16, Figure 1) corresponding to one of the two lipid tails.

As shown in Figure 9, the DPPC−CH_2 is not close to the NH_3 group of the DPPS and, for the other two cases studied, the charge bridges with the phosphate oxygen prevail over the oxygen of the carbonyl group.

3.2. DPPC Headgroup Orientation. To gain insight into the lipid headgroup orientation, the angle θ was defined as the angle between the **P**−**N** vector of the lipid heads and the outward normal of each leaflet. Figure 10 depicts the angle distribution function of the system studied. The leaflet composed only of DPPC without $DPPS^-$ is called leaflet 1, while the leaflet containing DPPS is called leaflet 2.

In agreement with previous reports by Pandit et al.[4] and Sach et al.,[7] the **P**−**N** angle is almost parallel to the membrane surface in all cases. The values in Table 1 show that both leaflets in the asymmetric membrane present a reduction of 5° in the tilt

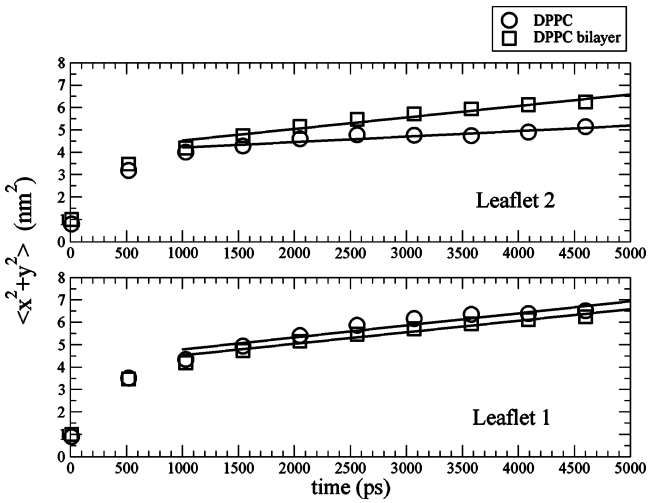

Figure 11. Parallel displacements of the DPPC molecules with respect the membrane plane on both leaflets. Leaflet 1 corresponds to the lipid layer without DPPS, and leaflet 2 corresponds to that with DPPS.

TABLE 1: Mean Angle Between the Vector Joining the P−N of the DPPC Lipid Headgroup and the Outward Normal to the Lipid Bilayer

	leaflet 1	leaflet 2
DPPC bilayer	84.64	84.72
with DPPS	82.22	80.55

of the **P**−**N** vector compared with the angle for the symmetrical DPPC membrane. From our results, we can assert that the reorientation of the head lipid is hardly affected by the presence of DPPS. This can be considered as further evidence that simulation artifacts play no role in the results obtained from these simulations.

3.3. Translation Diffusion Coefficient. The translational diffusion coefficient D_t can be calculated from the mean of the free square displacement defined as

$$\langle x^2 + y^2 \rangle = 4D_t^{lat} t$$
$$\langle z^2 \rangle = 2D_t^{tranv} t \qquad (5)$$

where the x and y axes correspond to the axes on the membrane plane and the z axis is perpendicular to the membrane plane. However, in the case of a bilayer, free displacement can only be considered in the $x-y$ plane. The translational diffusion coefficient along the z axis is not relevant in these simulations because it does not fit to the explicit condition imposed by eq 5.

Figure 11 depicts the correlation displacement of DPPC in the two leaflets of the asymmetric membrane, compared with a symmetric DPPC bilayer. From the slope of each curve, discarding the first 1000 ps where rapid motions associated with vibrations around an equilibrium point take place, rather than diffusive processes, we are able to estimate the translational diffusion coefficient of DPPC. Table 2 shows the calculated diffusion coefficients.

The data show that for DPPC, in the leaflet without DPPS, the translational diffusion coefficient is not perturbed unlike a bilayer of pure DPPC. On the other hand, the diffusion of DPPC in the leaflet with DPPS increases to 1.19×10^{-6} cm^2/s. In the case of DPPS diffusion, a value of 2.6×10^{-6} cm^2/s was measured, representing a slight diminution in the diffusion coefficient compared with the value obtained for a bilayer formed only of DPPS, 3.6×10^{-6} cm^2/s.[2] Even though these

TABLE 2: Translational Diffusion Coefficient in cm^2/s Parallel to the Membrane Plane[a]

	DPPC		DPPS
	leaflet 1	leaflet 2	leaflet 2
with DPPS	1.98×10^{-6}	1.19×10^{-6}	2.6×10^{-6}
DPPC bilayer	1.25×10^{-6}		

[a] Leaflets 1 and 2 correspond to the monolayers without and with DPPS, respectively.

values are typically 1 order of magnitude higher than the experimental ones ($D_{xy} \sim 10^{-7}-10^{-8}$ cm^2/s),[8] we must consider the difference in temperature at which we performed our simulations.

Conclusions

In this work, we have carried out two molecular dynamics simulations of an equilibrated and stable model of an asymmetric DPPS/DPPC bilayer resembling a biological membrane. We were able to evaluate how the presence of the charged $DPPS^-$ lipids in a leaflet perturbs the structure and dynamic properties of the lipids placed on the other leaflet of the membrane.

From the simulation results obtained, we conclude that the anisotropy existing in this lipid model of a membrane is not propagated from one leaflet to the other, as can be seen from the lipid head orientation, translational diffusion coefficient, lipid head hydration, or hydrocarbon order parameters of the lipid tails of the DPPC placed on both leaflets. On the other hand, the order parameter of the DPPC in the leaflet containing DPPS, increased noticeably compared with the values measured from a bilayer of DPPC. Regarding the DPPS behavior, their order parameter remained almost invariable compared with the values measured from a bilayer of DPPS.

Finally, the presence of undesired simulation artifacts that perturb certain properties, such as the surface lipid area, the mass gradient across the lipid bilayer, order lipid parameters, and lipid head orientation on both leaflets can be discounted. Therefore, this model of an asymmetric lipid bilayer can be used for further studies of systems of great biophysical relevance, such as lipid−protein or anaesthetic molecules embedded in an asymmetric lipid membranes.

Acknowledgment. J.J.L.C. and T.F.O. acknowledge financial support from the Spanish Ministry of Education and the Fundación Séneca de la Región de Murcia through Projects BQU-2001/0477 and AR-8-0271/FS/02, respectively. B.D.S. acknowledges support from the NIIH (USA). We also wish to thank the staff of the computing center (SAIT) of the Politechnic University of Cartegna for technical support.

References and Notes

(1) Egberts, E.; Marrink, S. J.; Berendsen, H. J. C. *Eur. Biophys. J.* **1994**, *22*, 423−436.
(2) López Cascales, J. J.; García de la Torre, J.; Marrink, S.; Berendsen, H. *J. Chem. Phys.* **1996**, *7*, 2713−2720.
(3) López Cascales, J. J.; Berendsen, H. J. C.; García de la Torre, J. *J. Phys. Chem.* **1996**, *100* (21), 8621−8627.
(4) Pandit, S.; Bostick, D.; Berkowitz, M. *Biophys. J.* **2003**, *84*, 3743−3750.
(5) Pandit, S.; Bostick, D.; Berkowitz, M. *Biophys. J.* **2003**, *85*, 3120−3131.
(6) Mukhopadhyay, L. M. P.; Tieleman, D. *Biophys. J.* **2004**, *86*, 1601−1609.
(7) Sach, J.; Nanda, H.; Petrache, H.; Woolf, T. *Biophys. J.* **2004**, *86*, 3772−3782.
(8) Yeagle, P. L. In *The dynamics of membrane lipids*; Yeagle, P., Ed.; CRC Press: Boca Raton, FL, 1992; p 170.
(9) Nato, N.; Nakanishi, M.; Hirashima, N. *Biochemistry* **2002**, *41*, 8068−8074.
(10) Weitzman, J. *J. Biol.* **2004**, *3*, 1−4.
(11) Williamson, P.; Schlegel, R. *J. Biol.* **2004**, *3*, 5−8.
(12) Schlegel, R. A.; Williamson, P. *Cell Death Differ.* **2001**, *8*, 551−563.
(13) Boon, J.; Smith, B. *Curr. Opin. Chem. Biol.* **2002**, *6*, 749−756.
(14) Matsuzaki, K. *Biochim. Biophys. Acta* **1998**, *3*, 391−400.
(15) Berendsen, H.; Grigera, J.; Straatsma, T. *J. Phys. Chem.* **1987**, *91*, 6269−6271.
(16) Lindahl, E.; Hess, B.; van der Spoel, D. *J. Mol. Mod.* **2001**, *7*, 306−317.
(17) Berendsen, H.; van der Spoel, D.; van Drunen, R. *Comput. Phys. Commun.* **1995**, *91*, 43−56.
(18) Darden, T.; York, D.; Pedersen, L. *J. Chem. Phys.* **1993**, *98*, 10089−10092.
(19) Essmann, U.; Perea, L.; Berkowitz, M.; Darden, T.; Lee, H.; Pedersen, L. *J. Chem. Phys.* **1995**, *103*, 8577−8593.
(20) Berendsen, H. J. C.; Postma, J. P. M.; van Gunsteren, W. F.; DiNola, A.; Haak, J. R. *J. Chem. Phys.* **1984**, *8*, 3684−3690.
(21) Seelig, A.; Seelig, J. *Biochemistry* **1974**, *13* (23), 4839−4845.
(22) De Young, L. R.; Dill, K. A. *Biochemistry* **1988**, *27*, 5281−5289.
(23) Cevc, G.; Watts, A.; Marsh, D. *Biochemistry* **1981**, *20*, 4955−4965.
(24) Hauser, H.; Paltauf, F.; Shipley, G. G. *Biochemistry* **1982**, *21*, 1061−1067.
(25) de Vries, A.; Chandrassekhar, I.; van Gunsteren, W.; Hunenberg, P. *J. Phys. Chem. B* **2005**, *109* (23), 11643−11652.
(26) Nagle, J.; Tristram-Nagle, S. *Biochim. Biophys. Acta* **2000**, *1469*, 159−195.
(27) Phillips, M.; Williams, R.; Chapman, D. *Chem. Phys. Lipids* **1969**, *3*, 234−244.
(28) Janiak, M.; Small, D.; Shipley, G. *J. Biol. Chem.* **1979**, *13*, 6068−6078.
(29) van Buuren, A.; Berendsen, H. *Langmuir* **1994**, *10*, 1703−1713.
(30) Marrink, S. J.; Berendsen, H. J. C. *J. Phys. Chem.* **1994**, *98* (15), 4155−4168.
(31) Brown, M. F. *J. Phys. Chem.* **1982**, *3*, 1576−1599.
(32) Browning, J. L.; Seelig, J. *Biochemistry* **1980**, *19*, 1262−1270.